


RESEARCH ARTICLE

Motor progression marker for newly diagnosed drug-naïve patients with Parkinson's disease: A resting-state functional MRI study

Yanbing Hou¹ | Lingyu Zhang¹ | Ruwei Ou¹ | Qianqian Wei¹ | Xiaojing Gu¹ |
Kuncheng Liu¹ | Junyu Lin¹ | Tianmi Yang¹ | Yi Xiao¹ | Qiyong Gong² |
Huifang Shang¹ 

¹Department of Neurology, Laboratory of Neurodegenerative Disorders, National Clinical Research Center for Geriatrics, West China Hospital, Sichuan University, Chengdu, Sichuan, China

²Huaxi MR Research Center (HMRR), Department of Radiology, West China Hospital, Sichuan University, Chengdu, Sichuan, China

Correspondence

Huifang Shang, MD, Department of Neurology, Laboratory of Neurodegenerative Disorders, National Clinical Research Center for Geriatrics, West China Hospital, Sichuan University, Chengdu 610041, Sichuan, China.
Email: hfshang2002@126.com

Qiyong Gong, PhD, Huaxi MR Research Center (HMRR), Department of Radiology, West China Hospital, Sichuan University, Chengdu 610041, Sichuan, China.
Email: huaxigongqy@163.com

Funding information

1.3.5 project for disciplines of excellence, West China Hospital, Sichuan University, Grant/Award Number: ZYJC18038; National Key Research and Development Program of China, Grant/Award Number: 2021YFC2501203

Abstract

The effective early prediction of clinical outcomes of Parkinson's disease (PD) is of great significance in the implementation of appropriate interventions. We aimed to propose a method based on the use of baseline resting-state functional characteristics (i.e., fractional amplitude of low-frequency fluctuations, fALFF) to predict motor progression in PD patients. Resting-state functional magnetic resonance imaging was performed on 48 newly-diagnosed drug-naïve PD patients and 27 age- and sex-matched healthy controls (HCs). Two PD subgroups were defined with different annual increase of Unified PD Rating Scale Part III motor scores. Least absolute shrinkage and selection operator regression analysis was performed to explore the baseline region-functional indicators for PD discrimination as well as the predictors for future motor deficits. Two significant models composed of baseline fALFF values from cerebral subregions were proposed. The classification model that distinguished PD patients from HCs (area under the curve [AUC] = 0.897) showed the most significant imaging characteristics in the putamen and precentral gyrus. The other prediction model that evaluated the degree of future deterioration of motor symptoms in PD patients (AUC = 0.916) showed the most significant imaging characteristics in the superior occipital gyrus and caudate nucleus. Furthermore, the increased regional function in bilateral caudate nuclei was correlated with the lower annual increase in

Abbreviations: AUC, area under the curve; BG, basal ganglia; CSF, cerebrospinal fluid; CSTC, cortico-striato-thalamo-cortical; CV, cross validation; DARTEL, diffeomorphic anatomic registration through an exponentiated lie algebra algorithm; EPI, echo-planar-imaging; fALFF, fractional amplitude of low-frequency fluctuation; FDR, false discovery rate; FWE, family-wise error; FWHM, full-width at half-maximum; GM, gray matter; HARS, Hamilton anxiety rating scale; HC, healthy control; HDRS, Hamilton depression rating scale; HL, Hosmer-Lemeshow; H&Y, Hoehn & Yahr; LASSO, least absolute shrinkage and selection operator; LEDD, levodopa equivalent daily dosage; ML, machine learning; MNI, Montreal neurological institute; MoCA, Montreal cognitive assessment; MRI, magnetic resonance imaging; NMSS, non-motor symptoms scale; PD, Parkinson's disease; PD_{AR}, Parkinson's disease rigidity dominant; PD_{TD}, Parkinson's disease tremor dominant; PDQ-39, Parkinson's disease questionnaire 39; ReHo, regional homogeneity; ROC, receiver operating characteristic; ROI, region of interest; rs-fMRI, resting-state functional MRI; UPDRS, unified Parkinson's disease rating scale; WM, white matter.

This is an open access article under the terms of the [Creative Commons Attribution-NonCommercial-NoDerivs](https://creativecommons.org/licenses/by-nc-nd/4.0/) License, which permits use and distribution in any medium, provided the original work is properly cited, the use is non-commercial and no modifications or adaptations are made.

© 2022 The Authors. *Human Brain Mapping* published by Wiley Periodicals LLC.

motor deficits in all PD patients. The caudate nucleus might be the core region responsible for future motor deficits in newly-diagnosed PD patients, which may aid the development of disease progression preventive strategies in clinical practice.

KEYWORDS

functional MRI, least absolute shrinkage and selection operator, newly-diagnosed, Parkinson's disease, prognosis

1 | INTRODUCTION

Parkinson's disease (PD) is one of the most common neurodegenerative diseases. The number of Chinese patients with PD is estimated to increase to 4.94 million by 2030, which could account for half of the patients with PD worldwide (Dorsey et al., 2007). Affected individuals experience a range of motor impairments and various non-motor symptoms, and this results in a significantly negative impact on their quality of life and a mounting socioeconomic burden. Moreover, disease progression is associated with increasing disability and mortality (Bloem et al., 2021). Thus, the reliable detection of PD progression is essential for the development of appropriate interventions.

Based on the highly heterogeneous presentations in PD, different clinical subtypes have been proposed with diverse progression rates (Marras & Lang, 2013). A study on autopsy-confirmed patients with PD, published in 2019, showed that the diffuse malignant subtype at diagnosis was related to more rapid progression towards relevant clinical milestones (i.e., dementia, recurrent falls, and wheelchair dependence) and reduced survival (De Pablo-Fernandez et al., 2019). However, the subtype classification has been challenged because of its instability over the course of disease and remains far from providing individualized prognosis in clinical practice. Novel and powerful predictors would enable the early identification of individuals with rapidly progressing disease who require serious attention, facilitate the prognostic discussions with patients, and enable disease-modifying studies to determine effective treatment strategies. Nevertheless, reliable biomarkers of PD progression remain unavailable.

Pathologically, the cardinal characteristics of PD are neuronal loss in the nigrostriatal system and Lewy pathology, the primary component of which is α -synuclein (Dickson et al., 2009). The α -synuclein pathology may occur in a localized manner and propagate across interconnected networks through the brain, followed by the appearance of clinical symptoms (Goedert et al., 2017). Magnetic resonance imaging (MRI) can be used to objectively measure wide-spread consequent alterations in the cerebral structure and function, thus aiding the identification of biomarkers for monitoring PD progression. Resting-state functional MRI (rs-fMRI) can help to unravel the reorganization of neural pathways and functional disruptions before the occurrence of neuronal death or brain atrophy, which suggests its potential as an early and sensitive marker of the pathological process (Filippi et al., 2020). The fractional amplitude of low-frequency fluctuation (fALFF) analysis can be used to measure the power of low-frequency resting-state signals and determine the intensity of regional

spontaneous brain activity in each brain region within a network (Zou et al., 2008). A two-year longitudinal rs-fMRI study found that the fALFF values in the cerebellum were positively correlated with the unified PD rating scale (UPDRS) Part III scores and changes in the scores, which suggests that the cerebellum may play an important role in the motor progression of patients with PD (Hu et al., 2015). Combined with machine learning (ML) and fALFF, a prediction algorithm of UPDRS scores at future timepoints could be established, and robust statistical patterns could be captured (Nguyen et al., 2021). Findings from one of our previous studies also showed that the ALFF values may enable the prediction of the UPDRS Part III score at baseline (Hou et al., 2016). These findings demonstrated that ALFF values might provide sufficient information about neurobiological changes and hold prognostic value for patients with PD.

Notably, chronic dopamine replacement therapy can variably influence the functional activities of the whole brain (Berman et al., 2016), and a degree of inconsistency among previous studies may be attributed to the inclusion of patients with PD at different stages or states (i.e., ON/OFF medication or drug-naïve). Based on these observations, this study aimed to develop the distinction and prediction models by applying fALFF parameters and explore the potential predictive brain regions for future motor deficits in a cohort of newly-diagnosed drug-naïve patients with PD.

2 | PATIENTS AND METHODS

2.1 | Study population

Patients with PD recruited in our cohort were diagnosed at the Movement Disorders Outpatient Clinic of West China Hospital of Sichuan University according to the diagnostic criteria of the unified Kingdom PD society brain bank (Hughes et al., 1992). The diagnosis of PD was re-evaluated by the movement disorder society clinical diagnostic criteria for PD (MDS-PD Criteria) (Postuma et al., 2015) before the study commenced. Patients were included if they (1) were first diagnosed at our center (i.e., to be “newly-diagnosed”); (2) did not undergo anti-Parkinson treatment or were not administered other centrally acting drugs (i.e., to be “drug-naïve”); (3) were followed up at least once in a “practical off” state. Patients were excluded if they had (1) a history of other neurological or psychiatric diseases, head injury, and neurological surgery; (2) structural brain defects visible on T1- or T2- imaging. A group of age- and sex-matched healthy controls (HCs) were

included if they had (1) no history of neurological or psychiatric diseases; (2) no family history of PD; (3) normal brain structure. The study was approved by the Ethics Committee of West China Hospital, Sichuan University (No. 2015-236), and registered in the Chinese Clinical Trial Registry (No. ChiCTR1800020033). Written informed consent was obtained from all participants.

2.2 | Clinical assessments

Demographic and clinical data, including data on the age, sex, level of education, and disease duration of participants, were collected. Motor assessment for each patient was completed at baseline and at the follow-up visit in a “practical off” state (i.e., the patient was free from antiparkinsonian medication for at least 12 h before motor assessment) (Albanese et al., 2001). The levodopa equivalent daily dosage (LEDD) was calculated for each patient (Tomlinson et al., 2010). The severity of PD was assessed using the Hoehn & Yahr (H&Y) stage (Hoehn & Yahr, 1967) and UPDRS (Movement Disorder Society Task Force on Rating Scales for Parkinson's, 2003). The UPDRS can be used to assess the motor disability and calculate the tremor and non-tremor scores (Eggers et al., 2011). PD can be categorized as rigidity dominant (PD_{AR}), tremor dominant (PD_{TD}), and mixed subtypes (refer to the Supplementary Material for details). Non-motor symptoms were evaluated using the non-motor symptoms scale (NMSS) (9 domains) (Wang et al., 2009). The Hamilton depression rating scale (HDRS) (24 items) (Moberg et al., 2001) and Hamilton anxiety rating scale (HARS) (Hamilton, 1959) were used to assess the characteristics of depression and anxiety, respectively. Montreal cognitive assessment (MoCA) (Nasreddine et al., 2005) was used to assess the cognitive function. The PD questionnaire 39 (PDQ-39) (Jenkinson et al., 1995) was used to evaluate the quality of life of patients with PD.

An increase of 2.5–5.2 points in the UPDRS Part III score indicates a clinically significant difference in patients with PD (Shulman et al., 2010). The numeric indicator of prognosis was calculated to evaluate motor progression for each patient with PD (Ou, Wei, Hou, Zhang, Liu, Lin, Jiang, Zhao, et al., 2021b; Ou, Wei, Hou, Zhang, Liu, Lin, Jiang, Song, et al., 2021a). In the current study, a rapid progression of motor symptoms was defined by at least a 2.5-point annual increase in the UPDRS Part III score, and the slow progression of motor symptoms was defined by an increase of <2.5 points.

2.3 | MRI acquisition and preprocessing

All MRI examinations were performed on a 3.0 Tesla (T) MRI scanner (Tim Trio; Siemens Healthineers, Erlangen, Germany) equipped with an eight-channel head coil. Participants were instructed to lay comfortably in supine position with their eyes closed. The foam pad was used to reduce head movement, and ear plugs were used to minimize

noise interference. High-resolution T1-weighted data were acquired using a volumetric three-dimensional spoiled gradient recall sequence (refer to the Supplementary Material for details). The rs-fMRI data were acquired using an echo-planar-imaging (EPI) sequence with the following parameters: repetition time [TR] = 2000 ms, echo time [TE] = 30 ms, flip-angle [FA] = 90°, field of view [FOV] = 240 × 240 mm², matrix size = 64 × 64, voxel size = 3.75 × 3.75 × 5 mm³, slice thickness = 5 mm (no slice gap). The total 240 volumes with 30 axial slices in each brain volume were obtained for each participant.

The rs-fMRI data were processed using the Statistical Parametric Mapping software (SPM12, <https://www.fil.ion.ucl.ac.uk/spm-statistical-parametric-mapping/>) and Data Processing & Analysis for Brain Imaging toolkit (DPABI, <http://rfmri.org/DPABI>). The preprocessing steps included: removal of the first 10 time points, slice timing corrections, spatial realignment to the middle volume, spatial normalization into the standard Montreal Neurological Institute (MNI) space, resampling into 3 × 3 × 3 mm³ for each voxel, spatial smoothing with 6-mm full-width at half-maximum (FWHM) Gaussian kernel, detrending, and nuisance signal regression (including the Friston 24-parameters, white matter (WM) and cerebrospinal fluid (CSF) signals). The head motion parameters for all participants were <1.5 mm maximum displacement in the x, y, or z plane and <1.5° angular rotation about each axis.

The low frequency power for each voxel was measured by band-pass filtering at 0.01–0.08 Hz, and then the normalized measure, fALFF was obtained through dividing the low-frequency power by the standard deviation of the unfiltered signal. For normalization, the z-scores for fALFF were calculated for each subject.

2.4 | Statistical analysis and regression models

All statistical analyses were performed using SPM12, R version 3.6.3., and SPSS 22.0. To identify the differences in demographic and clinical data, continuous variables expressed as mean ± standard deviations were compared using the *t*-test (or Mann–Whitney U test for variables with an abnormal distribution), and categorical variables were compared using the χ^2 test or Fisher's exact test.

The voxel-based comparison of fALFF maps between the PD and HC groups was performed using a two-sample *t*-test with age and sex as covariates. The significance threshold was $p < 0.001$ at the voxel level, and the family-wise error (FWE) correction for multiple comparisons was performed at the cluster level ($p < 0.05$). Moreover, the less stringent threshold was used with $p < 0.005$ at the voxel level and $p < 0.05$ corrected by FWE correction at the cluster level. In the PD group, two-tailed Pearson correlation analyses were performed to assess the relationship between the characteristics of motor deficits at baseline and mean values extracted from the regions of interest (ROIs).

The brain was divided into 116 cortical and subcortical ROIs using the automated anatomic labeling atlas (Tzourio-Mazoyer et al., 2002),

and the fALFF values for each ROI were extracted for each participant. To achieve the most critical imaging characteristics for distinguishing patients with PD from HCs, least absolute shrinkage and selection operator (LASSO) regression analysis was performed in this study. LASSO regression is a method of regression analysis that can be used to identify variables, estimate corresponding regression coefficients, and establish a model with minimized error. This method can be used to address problems of overfitting of variables and overestimation of the performance of the model in explaining variability. However, the regression coefficients may not be reliably interpretable in terms of independent risk factors (Ranstam & Cook, 2018). Ten-fold cross validation (CV) was used to determine the strength λ of the penalty term in LASSO. The minimum of the CV error was considered to produce the optimal value of λ . Through the LASSO analysis, the high dimensional imaging variables were resampled 1000 times, which could automatically remove unrelated covariates and show the most stable imaging characteristics. A classification model was constructed using the LASSO regression method. In addition, the LASSO regression analysis was performed to define the most critical imaging characteristics for distinguishing patients with PD with rapid motor progression from patients with PD with slow motor progression.

Receiver operating characteristic (ROC) curve analysis was performed to evaluate the sensitivity and specificity of the model. Moreover, the testing sets were randomly sampled from the whole cohort in the model for discriminating patients with PD (47 times, sample size ranging from 28 to 74 individually) and in the model for discriminating patients with PD with rapid motor progression (24 times, sample size ranging from 24 to 47 individually), following which the area under the ROC curve was evaluated in different random samples. The calibration plot was established to validate the model accompanied with the Hosmer-Lemeshow (HL) test.

The significant imaging characteristics identified from the first discrimination model were compared between patients with PD and HCs, and the characteristics from the second prediction model were compared between the two PD subgroups using the Wilcoxon rank-sum test. Multiple comparisons with false discovery rate (FDR) correction were performed. In addition, partial correlation analyses between imaging features and the characteristics of motor progression were calculated for all patients with PD, with the baseline UPDRS Part III scores and LEDD as covariates.

2.5 | Voxel-based morphometry analysis

Diffeomorphic anatomic registration through an exponentiated Lie algebra algorithm (DARTEL) was used to improve the registration of MR images that were segmented into the gray matter (GM), WM, and CSF (refer to the Supplementary Material for details). The voxel-based comparison of GM volume was performed between the PD and HC groups using a two-sample *t*-test with age and sex as covariates. The significance threshold was set at voxel-wise $p < 0.001$ and the cluster level of $p < 0.05$ corrected by FWE correction.

3 | RESULTS

3.1 | Baseline clinical characteristics

No significant difference was observed between patients with PD and HCs with respect to their age and sex. The mean disease duration of the enrolled drug-naïve patients with PD was 2.21 ± 2.01 years, with a mean UPDRS Part III score of 21.04 ± 8.04 . Three motor subtypes (PD_{AR}, PD_{TD}, and mixed subtypes) were identified with a substantial portion of the mixed subtype. Compared to the PD subgroup with a greater annual increase in motor deficits, the PD subgroup with a lesser annual increase in motor deficits showed a higher UPDRS Part I score. No significant differences were observed in the age, sex, education, disease duration, UPDRS Part II and III scores, H&Y stage, NMSS score, HDRS/HARS score, MoCA score, and quality of life between the two PD subgroups at baseline (Table 1).

3.2 | Longitudinal clinical characteristics

At follow-up, the mean disease duration of patients with PD was 4.25 ± 2.81 years, with a mean UPDRS Part III score of 28.40 ± 10.52 . The PD subgroup with a greater annual increase in motor deficits had higher UPDRS Part I, III, and IV scores and NMSS score compared to the subgroup with a lesser annual increase in motor deficits. No significant differences were observed in the LEDD, disease duration, UPDRS Part II score, H&Y stage, HDRS/HARS score, MoCA score, and quality of life between the two PD subgroups at follow-up visit (Table 1).

3.3 | Regional function in patients with PD

Upon comparison of the whole-brain fALFF maps between the PD and HC groups, the PD group was found to have a significantly lower fALFF value in the precentral and postcentral gyri, cuneus, lingual gyrus, and thalamus but a significantly elevated fALFF value in the superior and middle frontal gyri (Figure 1a and Table S1). Moreover, the reduced regional function in the precentral and postcentral gyri was correlated with more severe motor symptoms (UPDRS Part III scores) at baseline (Figure 1b and Table S2). After the significance threshold was relaxed, we further found that the PD group had a significantly lower fALFF value in the putamen (Table S3).

3.4 | Imaging characteristics-related models

3.4.1 | The classification model used to distinguish between patients with PD and HCs

Using the LASSO regression analysis, the classification model was constructed using the imaging characteristics from nine subregions, including the superior and middle frontal gyri, precentral and

TABLE 1 Demographic and clinical characteristics of PD patients and HCs at baseline and follow-up

Parameters	HC		All PD patients		PD patients with less than a 2.5-point annual increase in the UPDRS part III score		PD patients with at least a 2.5-point annual increase in the UPDRS part III score		P ¹ (HC vs. PD)	P ² (PD ^a vs. PD ^b)	P ³ (PD ^c vs. PD ^e)	P ⁴ (PD ^d vs. PD ^f)
	Baseline	Follow-up ^b	Baseline ^a	Follow-up ^b	Baseline ^c	Follow-up ^d	Baseline ^e	Follow-up ^f				
Number, n	27	48	48	48	23	23	25	25	-	-	-	-
Handedness of writing (R: L)	27:0	48:0	48:0	48:0	23:0	23:0	25:0	25:0	-	-	-	-
Age, years	51.28 ± 8.22	52.37 ± 10.12	52.37 ± 10.12	-	52.89 ± 8.72	-	51.88 ± 11.42	-	0.636	-	0.733	-
Sex, M/F	12/15	29/19	29/19	-	11/12	-	18/7	-	0.137	-	0.087	-
EDU, years	-	10.54 ± 3.43	10.54 ± 3.43	-	10.04 ± 3.05	-	11.00 ± 3.74	-	-	-	0.233	-
Duration of disease, years	-	2.21 ± 2.01	2.21 ± 2.01	4.25 ± 2.81	2.20 ± 1.77	4.49 ± 2.54	2.22 ± 2.25	4.03 ± 3.07	-	-	0.433	0.270
LEDD	-	-	314.22 ± 213.45	-	301.61 ± 217.13	-	325.82 ± 213.81	-	-	-	-	0.568
H & Y stage	-	1.85 ± 0.48	1.85 ± 0.48	2.06 ± 0.34	1.85 ± 0.35	1.86 ± 0.59	2.02 ± 0.18	2.10 ± 0.43	-	0.001*	0.615	0.711
UPDRS score	-	-	-	-	-	-	-	-	-	-	-	-
Part I	-	0.90 ± 1.46	0.90 ± 1.46	1.17 ± 1.45	1.30 ± 1.74	0.74 ± 1.21	0.52 ± 1.05	1.56 ± 1.56	-	0.296	0.042*	0.024*
Part II	-	6.21 ± 3.93	6.21 ± 3.93	8.83 ± 4.87	6.22 ± 3.34	7.43 ± 4.12	6.20 ± 4.47	10.12 ± 5.21	-	<0.001*	0.988	0.055
Part III	-	21.04 ± 8.04	21.04 ± 8.04	28.40 ± 10.52	22.04 ± 6.78	24.17 ± 7.22	20.12 ± 9.09	32.28 ± 11.67	-	<0.001*	0.414	0.006*
Part IV	-	-	-	0.25 ± 0.96	-	0.00 ± 0.00	-	0.48 ± 1.29	-	-	-	0.048*
Motor phenotype (TD/AR/Mixed)	-	3/16/29	3/16/29	0/22/26	1/6/16	0/10/13	2/10/13	0/12/13	-	-	0.454	0.753
NMSS score	-	20.79 ± 17.10	20.79 ± 17.10	21.42 ± 19.50	24.43 ± 20.80	16.04 ± 17.96	17.44 ± 12.32	26.36 ± 19.89	-	0.731	0.489	0.014*
HDRS score	-	5.00 ± 5.48	5.00 ± 5.48	6.29 ± 6.26	5.61 ± 6.58	5.13 ± 6.68	4.44 ± 4.31	7.36 ± 5.78	-	0.065	0.739	0.070
HARS score	-	3.85 ± 4.31	3.85 ± 4.31	4.96 ± 5.85	4.78 ± 4.99	4.65 ± 6.52	3.00 ± 3.45	5.24 ± 5.29	-	0.246	0.135	0.567
MoCA score	-	26.50 ± 2.84	26.50 ± 2.84	26.21 ± 3.45	26.74 ± 2.32	26.91 ± 2.76	26.28 ± 3.27	25.56 ± 3.93	-	0.696	0.967	0.311
PDQ-39 score	-	19.19 ± 15.13	19.19 ± 15.13	21.48 ± 19.76	18.87 ± 14.46	16.30 ± 11.98	19.48 ± 16.01	26.24 ± 24.16	-	0.537	0.820	0.307

Note: *Indicates significant difference. ¹Comparison between all PD patients and HCs. ²Comparison between all PD patients at baseline and follow-up. ³Comparison between PD subgroups at baseline.

⁴Comparison between PD subgroups at follow-up.

Abbreviations: AR, akinetic rigidity; EDU, education; F, female; HARS, Hamilton anxiety rating scale; HC, healthy control; HDRS, Hamilton depression rating scale; H & Y, Hoehn & Yahr; L, left; LEDD, levodopa equivalent daily dosage; M, male; MoCA, Montreal cognitive assessment; NMSS, non-motor symptom scale; PD, Parkinson's disease; PDQ-39, 39-item PD questionnaire; R, right; TD, tremor dominant; UPDRS, unified PD rating scale.

^aall PD patients at baseline.

^ball PD patients at follow-up.

^cPD patients with less than 2.5-point annual increase of the UPDRS-III score at baseline.

^dPD patients with less than 2.5-point annual increase of the UPDRS-III score at follow-up.

^ePD patients with at least 2.5-point annual increase of the UPDRS-III score at baseline.

^fPD patients with at least 2.5-point annual increase of the UPDRS-III score at follow-up.

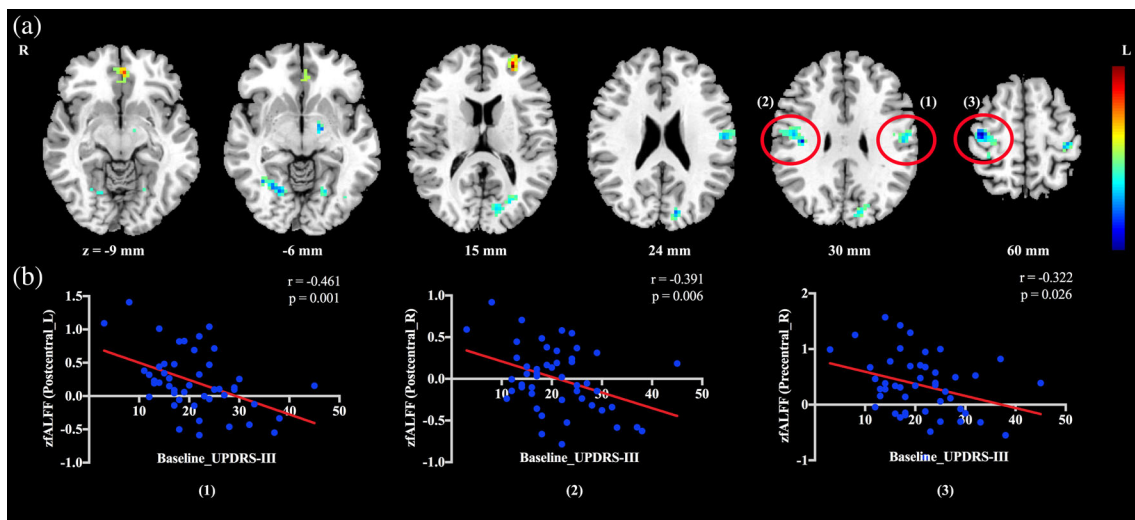


FIGURE 1 (a) The PD group showed a higher fALFF value in the middle frontal ($z = -9$ mm), left superior frontal ($z = 15$ mm) areas and a lower fALFF value in the left thalamus ($z = -6$ mm), bilateral lingual gyri ($z = -6$ mm and 15 mm), left cuneus ($z = 24$ mm), and bilateral sensorimotor regions ($z = 30$ mm and 60 mm), compared with the HC group. (b) The scatterplots showed the significantly negative correlations between the baseline UPDRS part III motor scores and the mean fALFF values in the bilateral sensorimotor regions of all patients with PD. Abbreviations: fALFF, fractional amplitude of low-frequency fluctuations; HC, healthy control; L, left; PD, Parkinson's disease; R, right; UPDRS-III, unified PD rating scale part III

postcentral gyri, inferior temporal gyrus, inferior cerebellum, and putamen (Figure 2a,b; Table S4). The coefficients of each variable in this model are displayed in Figure 2c and Table S4. Notably, the imaging characteristics of the right putamen and right precentral gyrus showed the highest coefficients. With respect to the performance of this model, the area under the curve (AUC) was 0.897 (95% CI: 0.828–0.967). In detail, the sensitivity and specificity were 75.0% and 92.6%, respectively, and the cutoff value was 0.65 (Figure 2d). The randomly sampled internal dataset was further used to test the capability of this model. As shown in Figure 2e, all the AUCs were fluctuated around the AUC of the model, indicating a good predictive ability. The calibration curves indicated good probability consistencies (Figure 2f) and the HL goodness-of-fit test showed no significant deviation between the observed and predicted events ($p = 0.886$).

3.4.2 | The prediction model for patients with PD with rapid motor progression

Using the same method as mentioned above, the prediction model was constructed using imaging characteristics from 12 subregions, including the inferior frontal gyrus, olfactory cortex, hippocampus, temporal pole, superior occipital gyrus, superior and inferior cerebellum, thalamus, caudate nucleus, and putamen (Figure 3a,b; Table S4). The coefficients are displayed in Figure 3c; Table S4. The imaging characteristics of the right superior occipital gyrus and bilateral caudate nuclei showed the highest coefficients. With respect to the predictive power, the AUC was 0.916 (95% CI: 0.834–0.999). The sensitivity and specificity were 100.0% and 87.0%, respectively. The

cutoff value was 0.50 (Figure 3d). As shown in Figure 3e, the model yielded a good performance. The calibration curves also indicated good probability consistencies (Figure 3f), and the HL test did not yield significant deviation between the observed and predicted events ($p = 0.198$).

3.4.3 | Post-hoc ROI analysis

Significant imaging characteristics from the abovementioned models were compared between the two groups. Relative to the HCs, patients with PD showed a significantly reduced fALFF value in the putamen and sensorimotor regions and a significantly elevated fALFF value in frontal and temporal areas (Figure 4a). In addition, relative to patients with PD with rapid motor progression, patients with PD with slow motor progression had a significantly lower fALFF value in the superior occipital gyrus, but a significantly greater fALFF value in the caudate nucleus, hippocampus, and the inferior frontal region (Figure 4b).

3.4.4 | Association between the regional function and motor progression

The results of the partial correlation analyses are shown in Figure 4c. In the PD group, the significant negative correlation was observed between the fALFF value in the bilateral caudate nuclei and the annual increase in the UPDRS Part III score (right caudate nucleus: $r = -0.345$; $p = 0.019$; left caudate nucleus: $r = -0.344$; $p = 0.019$).

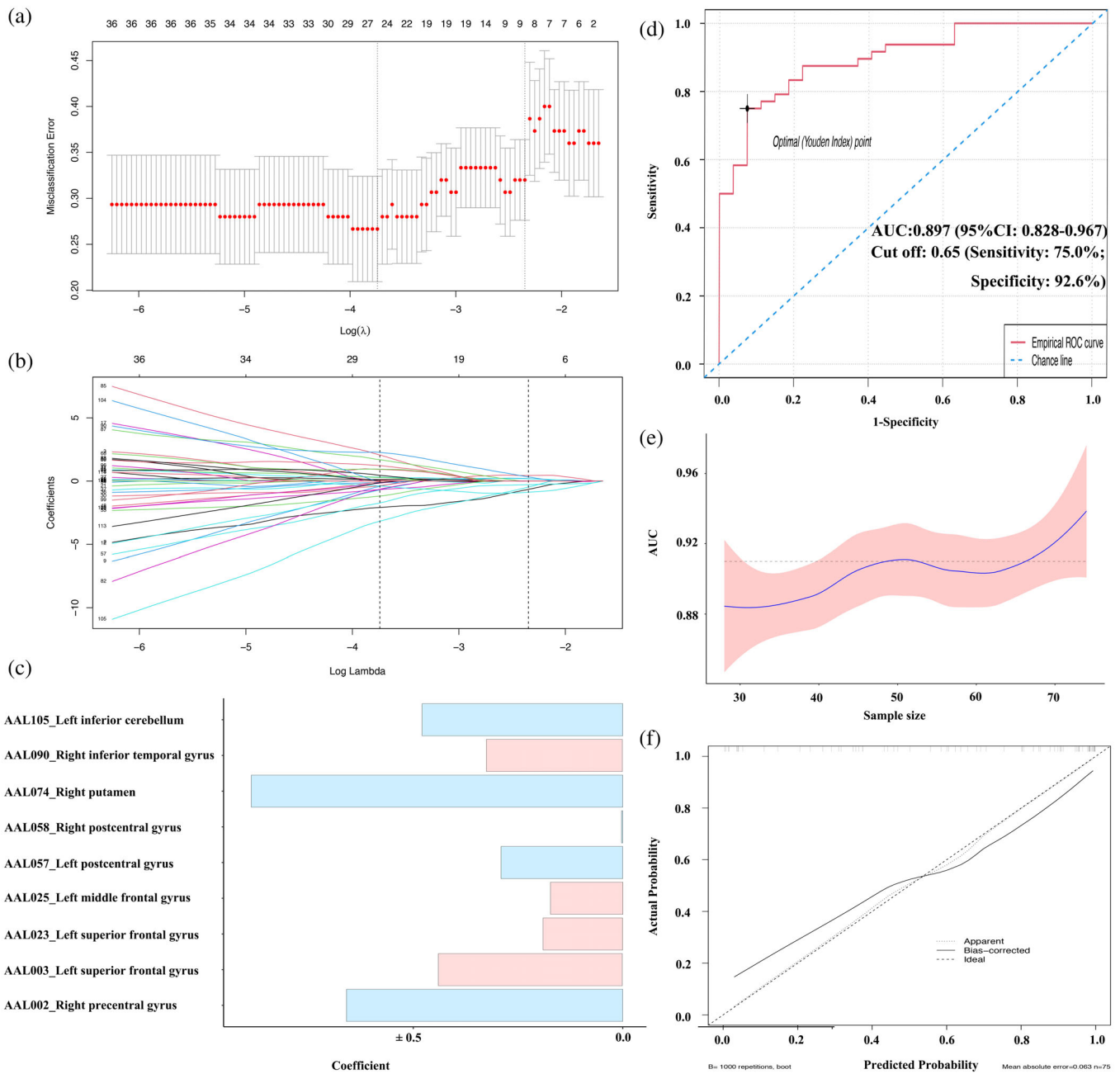


FIGURE 2 Establishment of the classification (PD patients vs. HCs) model using LASSO regression with a 10-fold cross-validation (a), counting the minimum criteria (λ) (b), and corresponding coefficients (c). (d) The ROC curves for the distinction of patients with PD from HCs. (e) Internal validation of the model. The testing sets were randomly sampled from the whole cohort by 47 times, ranging from 28 to 74 performed individually, following which the area under the ROC curve with 95% confidence intervals was evaluated in different random samples. (f) Calibration plots of the classification model. Abbreviations: AAL, automated anatomic labeling; AUC, area under the curve; HC, healthy control; LASSO, least absolute shrinkage and selection operator; PD, Parkinson's disease; ROC, receiver operating characteristic

3.4.5 | VBM analysis

We did not observe any significant difference in the GM volume between the PD and HC groups, which indicated the absence of robust association between the altered regional function and anatomic changes in the cohort of newly-diagnosed drug-naïve patients with PD.

4 | DISCUSSION

In the current study, we investigated the resting-state regional spontaneous neuronal activity in a cohort of newly-diagnosed drug-naïve patients with PD. Additionally, we explored the baseline region-functional indicators for the discrimination of PD and the predictors for future motor deficits in PD. Overall, our key findings were: (1) The

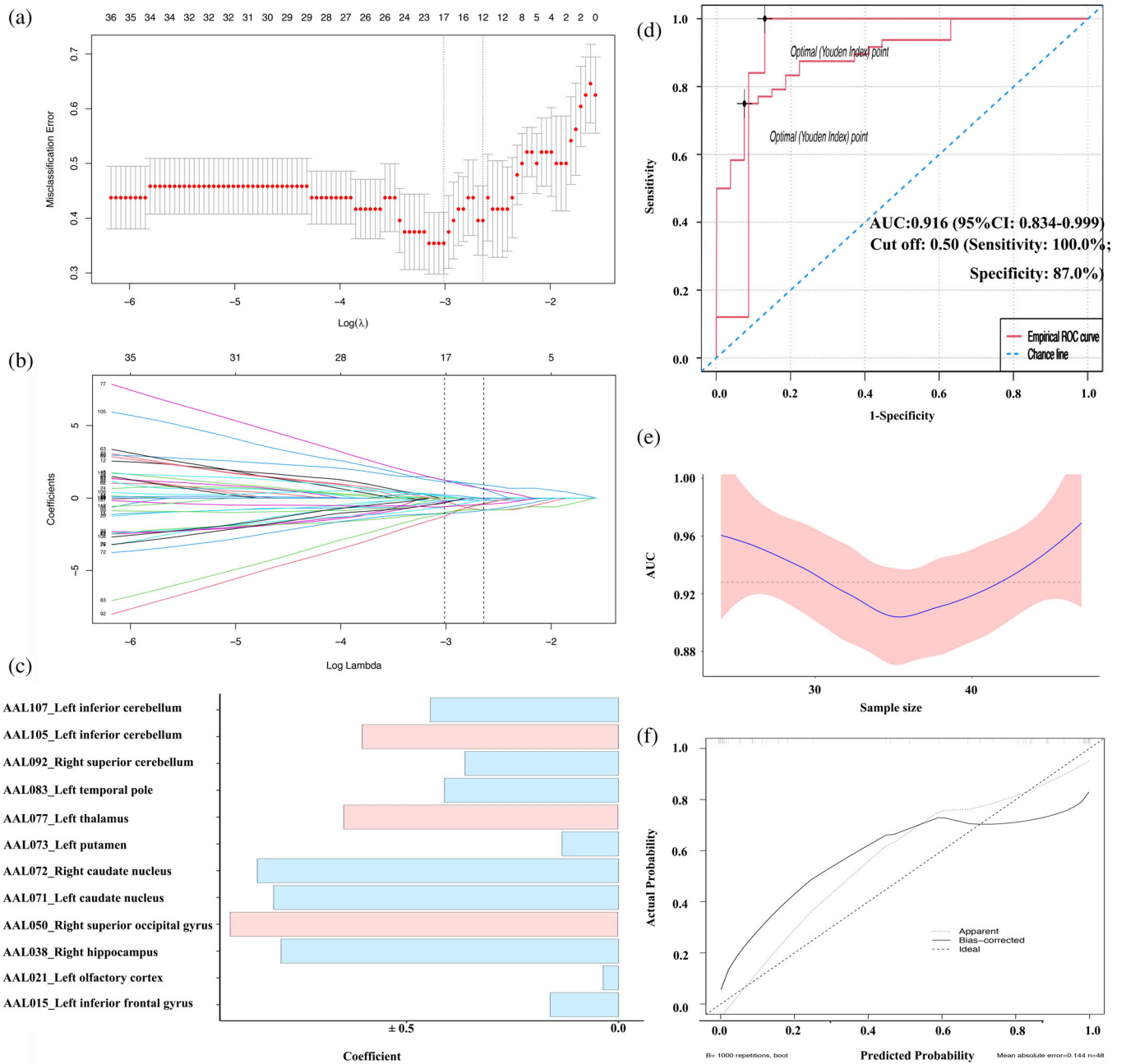
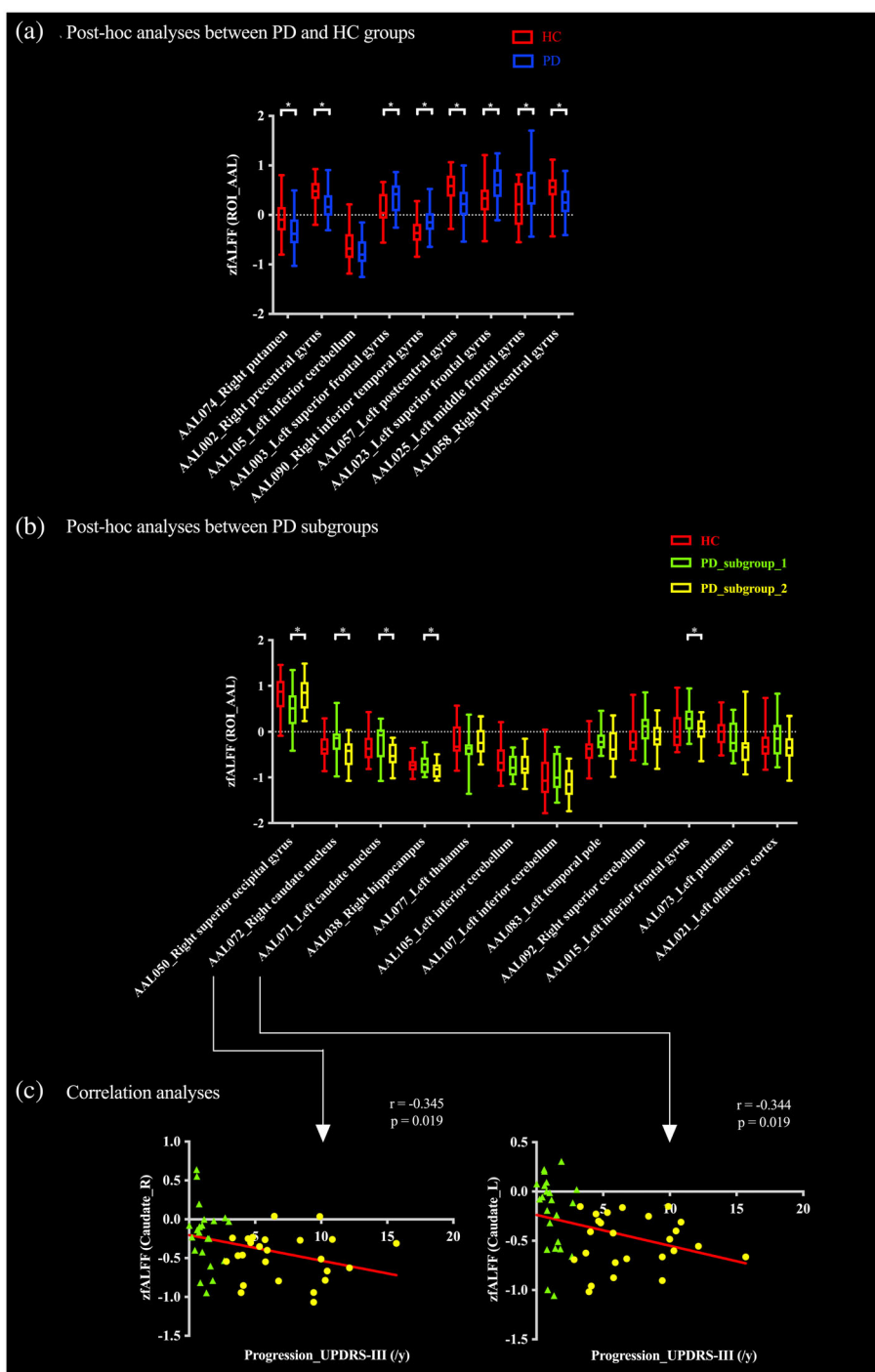


FIGURE 3 Establishment of the prediction (PD patients with rapid or slow motor progression) model using LASSO regression with a 10-fold cross-validation (a), counting the minimum criteria (λ) (b), and corresponding coefficients (c). (d) The ROC curves for the evaluation of the potential degree of deterioration of motor symptoms in patients with PD. (e) Internal validation of the model. The testing sets were randomly sampled from the whole cohort by 24 times, ranging from 24 to 47 performed individually, following which the area under the ROC curve with 95% confidence intervals was evaluated in different random samples. (f) Calibration plots of the prediction model. Abbreviations: AAL, automated anatomic labeling; AUC, area under the curve; LASSO, least absolute shrinkage and selection operator; PD, Parkinson's disease; ROC, receiver operating characteristic

voxel-based analysis revealed the presence of significantly impaired spontaneous neuronal activities in the superior and middle frontal areas, sensorimotor region (precentral and postcentral gyri), occipital subregions (cuneus and lingual gyrus), thalamus, and putamen in patients with PD relative to HCs. The abnormal regional function of the sensorimotor region was correlated with the motor symptoms of patients with PD at baseline. (2) Two significant models composed of

baseline fALFF values from the cerebral subregions were proposed. The classification model used for distinguishing patients with PD from HCs showed the most significant imaging characteristics in the putamen and precentral gyrus. The other prediction model used for evaluating the degree of potential future deterioration in the motor symptoms of patients with PD showed the most significant imaging characteristics in the superior occipital gyrus and caudate nucleus.

FIGURE 4 (a) Regional mean fALFF values in the PD and HC groups. Significantly altered fALFF values between the two groups were observed in eight ROIs ($*p < 0.05$, FDR corrected). (b) Regional mean fALFF values in the HC and two PD subgroups. Significantly altered fALFF values between the two PD subgroups were observed in five ROIs ($*p < 0.05$, FDR corrected). The PD_subgroup_1 refers to the PD subgroup with a lower annual increase in motor deficits, and the PD_subgroup_2 refers to the PD subgroup with a higher annual increase in motor deficits. (c) Scatterplots showed the significantly negative partial correlations between the annual increase in the UPDRS part III motor scores and the mean fALFF values in the bilateral caudate nuclei in all patients with PD. Abbreviations: fALFF, fractional amplitude of low-frequency fluctuations; HC, healthy control; L, left; PD, Parkinson's disease; R, right; ROI, region of interest; UPDRS-III, unified PD rating scale part III



(3) The higher spontaneous neuronal activities in the bilateral caudate nuclei were correlated with the lower annual increase in motor deficits in all patients with PD, suggesting that the caudate nucleus might be the core predictor for future motor deficits in newly-diagnosed patients with PD, thereby promoting a deeper understanding of the potential mechanisms underlying the deterioration of motor symptoms in PD.

The pathological hallmark of PD is dopamine neuronal loss in the substantia nigra pars compacta of the basal ganglia (BG) (Braak et al., 2003), which can regulate cortical function through the cortico-

striato-thalamo-cortical (CSTC) circuits (Albin et al., 1989; Alexander et al., 1986; DeLong et al., 1984). The classic model implicated in cardinal motor impairments of patients with PD comprises the dysfunction of CSTC circuits (Galvan & Wichmann, 2008). In the voxel-based analysis, we found that patients with PD showed local spontaneous neuronal hypoactivity in the putamen, thalamus, sensorimotor region, occipital subregions, and hyperactivity in the frontal subregions relative to HCs, a finding that was consistent with the findings from other studies on patients with PD (Li et al., 2020; Luo et al., 2015; Possin et al., 2013; Zhang et al., 2013). Indeed, the decreased regional

function in the putamen and precentral gyrus were the most consistent features in patients with PD, as indicated by evidence from previous meta-analyses (Jia et al., 2021; Pan et al., 2017; Wang, Jia, et al., 2018). The dopamine neuronal loss from the substantia nigra in PD leads to dopamine expenditure in the striatum, particularly in the putamen. We also observed that the lower local function in the sensorimotor region was correlated with the baseline motor symptoms of patients with PD, which might reflect the pathophysiological mechanism of motor impairments. The occipital region containing multiple anatomical regions of the visual cortex is crucial to the processing of visual information and the generation of motor plans (Meppelink et al., 2009). The reduced regional function in the cuneus and lingual areas indicated that patients with PD may suffer from impairment of visual processing early on before the onset of clinically visual symptoms (e.g., visual hallucinations). The largest part of the frontal region is the prefrontal cortex, which plays important roles in many domains of cognitive function, such as executive function, attention, and memory (Gabrieli et al., 1998; Miller & Cohen, 2001; Yuan & Raz, 2014). Findings from previous studies have shown that the more severe cognitive deficits induced stronger neural activity in the frontal region, thus suggesting an adaptive compensatory effect in response to a modest cognitive decline in early PD (Nagano-Saito et al., 2016; Wang, Zhang, et al., 2018). The enhanced regional function in the frontal subregions observed in our study may also reflect a compensatory mechanism; however, this warrants further investigation.

We used the imaging characteristics from rs-fMRI to discriminate between samples collected from patients with PD and HCs and predict potential motor deficits in patients with PD. In two recent studies, measures derived from rs-fMRI were used to predict PD prognosis. Nguyen et al. (2021) used baseline measures including regional homogeneity (ReHo) and fALFF, to predict the future on-medication UPDRS scores for patients with PD, which focused on the total score rather than the UPDRS Part III motor score that can be more severely influenced by dopaminergic treatment. De Micco et al. (2021) stratified drug-naïve patients with PD into two subtypes (early/mild and early/severe) at baseline, explored the association between the baseline topologic metrics and clinical changes, and only observed significant correlations between the functional topological metrics and cognitive progression. No significant correlation was observed between the imaging metrics at baseline and motor progression. Other imaging measures (e.g., atrophy pattern or diffusion property) have been evaluated to predict the progression trajectories of motor function in drug-naïve patients with PD (Abbasi et al., 2020; Burciu et al., 2017; Zeighami et al., 2019). Converging evidence suggests that functional alterations in the brain can be detectable before the occurrence of brain atrophy, especially in the early stage of the disease (Luo et al., 2014). Biomarkers obtained from rs-fMRI may have greater power to indicate disease prognosis in drug-naïve patients with PD and contribute to a larger extent to the confidence of neurologists in the prognosis of PD at the initial diagnosis stage. In our study, two significant models (classification and prediction models) composed of the baseline fALFF values from cerebral regions were proposed with a high AUC of 0.897 and 0.916, respectively. These two models

indicated that the baseline fALFF from newly-diagnosed drug-naïve patients with PD may be used to confidently identify PD and presage early motor evolution in individuals.

The baseline fALFF values in the putamen, sensorimotor region, cerebellum, and frontal and temporal regions were indicators for PD discrimination, and participants from the PD group showed significantly lower fALFF values in the putamen and sensorimotor region and enhanced fALFF values in the frontal and temporal regions compared to HCs. In addition, the baseline fALFF values in more extensive cerebral regions were predictors for potential motor progression in PD, and the PD subgroup with slow motor progression showed significantly lower fALFF values in the superior occipital gyrus, and increased fALFF values in the caudate nucleus, hippocampus, and frontal region. Of note, the most significant characteristics of the two models were considerably different. The most significant imaging characteristics from the putamen and precentral gyrus in the classification model may reflect the pathophysiological changes in the development of PD-related symptoms, whereas the most significant imaging characteristics from the prediction model are worthy of further investigation.

As widely known, the key symptom of motor deficits in PD does not develop until 50%–60% of nigral dopaminergic neurons are lost (Fearnley & Lees, 1991), which reflects the capacity of an individual to tolerate neuropathological lesions and is known as the neural reserve. However, the suggested motor reserve is different among patients with PD, which may explain the individual heterogeneity in parkinsonian motor signs at similar levels of pathological changes (Chung, Lee, et al., 2020). This implies that patients with PD with a greater motor reserve may have milder motor deficits than striatal dopamine loss. A previous rs-fMRI study identified a motor reserve network for patients with PD, including the BG (i.e., putamen, caudate nucleus, and pallidum), inferior frontal cortex, insula, cerebellum, hippocampus, and amygdala (Chung, Kim, et al., 2020). The increased functional connectivity within the motor reserve network indicated a greater motor reserve in patients with PD. Moreover, the higher connectivity strength within the network was correlated with the slower rate of longitudinal increase in dopaminergic medication doses, that suggesting a significant association with motor progression and the ability to cope with neurodegeneration throughout disease progression in PD.

We identified several regions, such as the BG (i.e., putamen and caudate nucleus), hippocampus, cerebellum, and inferior frontal region, had predictive value in the progression of motor deficits. Specifically, the bilateral caudate nuclei, right hippocampus, and left inferior frontal region showed significantly enhanced regional function in the PD subgroup with a lower rate of annual increase in motor deficits relative to the PD subgroup with a higher rate of annual increase. Moreover, the core predictive features from the bilateral caudate nuclei were significantly negatively correlated with the annual increase in the UPDRS Part III motor scores. These findings supported the recent concept of motor reserve, and suggested that bilateral caudate nuclei might be the key region responsible for the progression of motor deficits as well as the core targets for preventive strategies of disease progression for newly-diagnosed drug-naïve patients with PD.

The current study had certain limitations. The generalizability of the study findings might be limited by the relatively small sample size of patients with PD. This limitation was partly attributable to the strict quality control, such as the drug-naïve status of patients with PD at baseline and in the off-medication state at the follow-up visit, which was the primary advantage of the study. Nevertheless, further investigations with a larger sample size are warranted. Moreover, the external validation of these models should be conducted in the future. In addition, the proportion of male participants was greater in the PD subgroup with a higher rate of annual increase in motor deficits (72%) than in the PD subgroup which had a lower rate (47.8%), although the difference in the sex ratio was not significant ($p = 0.087$). The p value may not be adequately small, given the small sample size. To date, the role of sex in determining either a more aggressive or a more benign motor disease course is far from clear (Picillo et al., 2017). Findings from two recent longitudinal studies on large PD cohorts suggested that the sex-associated difference in the progression rate of motor impairments was minimal (Abraham et al., 2019; Iwaki et al., 2021). More studies need to be conducted to better understand sex-related differences in PD progression.

5 | CONCLUSIONS

Our findings revealed a resting-state regional spontaneous neuronal reorganization in newly-diagnosed drug-naïve patients with PD. Moreover, the findings of this study provided compelling evidence for the potential value of fALFF derived from rs-fMRI data in the distinction and prognostication of PD. Continued efforts to develop imaging-based predictive tools will not only improve clinical disease monitoring but also promote the development of more appropriate treatment strategies in clinical settings.

AUTHOR CONTRIBUTIONS

Yanbing Hou: (1) Research project: A. Conception, B. Organization, C. Execution; (2) Statistical Analysis: Design; (3) Manuscript: Writing of the first draft; **Lingyu Zhang and Ruwei Ou:** (1) Statistical Analysis: Review and Critique; (2) Patient enrollment; **Qianqian Wei, Xiaojing Gu, Kuncheng Liu, Junyu Lin, Tianmi Yang, and Yi Xiao:** Patient enrollment and follow-up; **Qiyong Gong and Huifang Shang:** (1) Research project: Conception; (2) Statistical Analysis: Review and Critique; (3) Manuscript: Review and Critique. All authors have read and approved the final manuscript.

ACKNOWLEDGMENT

The authors thank the patients and their families for their participation in the study.

FUNDING INFORMATION

This work was supported by the National Key Research and Development Program of China (2021YFC2501203 to H.F.S), and the 1.3.5 project for disciplines of excellence, West China Hospital, Sichuan University (ZYJC18038 to H.F.S).

CONFLICT OF INTEREST

The authors declare that they have no competing interests.

DATA AVAILABILITY STATEMENT

All data generated or analyzed during this study are available from the corresponding author by reasonable request.

ORCID

Huifang Shang  <https://orcid.org/0000-0003-0947-1151>

REFERENCES

- Abbasi, N., Fereshtehnejad, S. M., Zeighami, Y., Larcher, K. M., Postuma, R. B., & Dagher, A. (2020). Predicting severity and prognosis in Parkinson's disease from brain microstructure and connectivity. *Neuroimage: Clinical*, 25, 102111. <https://doi.org/10.1016/j.nicl.2019.102111>
- Abraham, D. S., Gruber-Baldini, A. L., Magder, L. S., McArdle, P. F., Tom, S. E., Barr, E., Schrader, K., & Shulman, L. M. (2019). Sex differences in Parkinson's disease presentation and progression. *Parkinsonism & Related Disorders*, 69, 48–54. <https://doi.org/10.1016/j.parkrelidis.2019.10.019>
- Albanese, A., Bonuccelli, U., Brefel, C., Chaudhuri, K. R., Colosimo, C., Eichhorn, T., Melamed, E., Pollak, P., Van Laar, T., & Zappia, M. (2001). Consensus statement on the role of acute dopaminergic challenge in Parkinson's disease. *Movement Disorders*, 16(2), 197–201. <https://doi.org/10.1002/mds.1069>
- Albin, R. L., Young, A. B., & Penney, J. B. (1989). The functional anatomy of basal ganglia disorders. *Trends in Neurosciences*, 12(10), 366–375. [https://doi.org/10.1016/0166-2236\(89\)90074-x](https://doi.org/10.1016/0166-2236(89)90074-x)
- Alexander, G. E., DeLong, M. R., & Strick, P. L. (1986). Parallel organization of functionally segregated circuits linking basal ganglia and cortex. *Annual Review of Neuroscience*, 9, 357–381. <https://doi.org/10.1146/annurev.ne.09.030186.002041>
- Berman, B. D., Smucny, J., Wylie, K. P., Shelton, E., Kronberg, E., Leehey, M., & Tregellas, J. R. (2016). Levodopa modulates small-world architecture of functional brain networks in Parkinson's disease. *Movement Disorders*, 31(11), 1676–1684. <https://doi.org/10.1002/mds.26713>
- Bloem, B. R., Okun, M. S., & Klein, C. (2021). Parkinson's disease. *Lancet*, 397(10291), 2284–2303. [https://doi.org/10.1016/S0140-6736\(21\)00218-X](https://doi.org/10.1016/S0140-6736(21)00218-X)
- Braak, H., Del Tredici, K., Rub, U., de Vos, R. A., Jansen Steur, E. N., & Braak, E. (2003). Staging of brain pathology related to sporadic Parkinson's disease. *Neurobiology of Aging*, 24(2), 197–211.
- Burciu, R. G., Ofori, E., Archer, D. B., Wu, S. S., Pasternak, O., McFarland, N. R., Okun, M. S., & Vaillancourt, D. E. (2017). Progression marker of Parkinson's disease: A 4-year multi-site imaging study. *Brain*, 140(8), 2183–2192. <https://doi.org/10.1093/brain/awx146>
- Chung, S. J., Kim, H. R., Jung, J. H., Lee, P. H., Jeong, Y., & Sohn, Y. H. (2020). Identifying the functional brain network of Motor Reserve in Early Parkinson's disease. *Movement Disorders*, 35(4), 577–586. <https://doi.org/10.1002/mds.28012>
- Chung, S. J., Lee, J. J., Lee, P. H., & Sohn, Y. H. (2020). Emerging concepts of Motor Reserve in Parkinson's disease. *Journal of Movement Disorders*, 13(3), 171–184. <https://doi.org/10.14802/jmd.20029>
- De Micco, R., Agosta, F., Basaia, S., Siciliano, M., Cividini, C., Tedeschi, G., Filippi, M., & Tessoro, A. (2021). Functional Connectomics and disease progression in drug-naïve Parkinson's disease patients. *Movement Disorders*, 36, 1603–1616. <https://doi.org/10.1002/mds.28541>
- De Pablo-Fernandez, E., Lees, A. J., Holton, J. L., & Warner, T. T. (2019). Prognosis and Neuropathologic correlation of clinical subtypes of

- Parkinson disease. *JAMA Neurology*, 76(4), 470–479. <https://doi.org/10.1001/jamaneurol.2018.4377>
- DeLong, M. R., Alexander, G. E., Georgopoulos, A. P., Crutcher, M. D., Mitchell, S. J., & Richardson, R. T. (1984). Role of basal ganglia in limb movements. *Human Neurobiology*, 2(4), 235–244.
- Dickson, D. W., Braak, H., Duda, J. E., Duyckaerts, C., Gasser, T., Halliday, G. M., Hardy, J., Leverenz, J. B., Del Tredici, K., Wszolek, Z. K., & Litvan, I. (2009). Neuropathological assessment of Parkinson's disease: Refining the diagnostic criteria. *Lancet Neurology*, 8(12), 1150–1157. [https://doi.org/10.1016/S1474-4422\(09\)70238-8](https://doi.org/10.1016/S1474-4422(09)70238-8)
- Dorsey, E. R., Constantinescu, R., Thompson, J. P., Biglan, K. M., Holloway, R. G., Kieburtz, K., Marshall, F. J., Ravina, B. M., Schifitto, G., Siderowf, A., & Tanner, C. M. (2007). Projected number of people with Parkinson disease in the most populous nations, 2005 through 2030. *Neurology*, 68(5), 384–386. <https://doi.org/10.1212/01.wnl.0000247740.47667.03>
- Eggers, C., Kahraman, D., Fink, G. R., Schmidt, M., & Timmermann, L. (2011). Akinetic-rigid and tremor-dominant Parkinson's disease patients show different patterns of FP-CIT single photon emission computed tomography. *Movement Disorders*, 26(3), 416–423. <https://doi.org/10.1002/mds.23468>
- Fearnley, J. M., & Lees, A. J. (1991). Ageing and Parkinson's disease: Substantia nigra regional selectivity. *Brain*, 114(Pt 5), 2283–2301. <https://doi.org/10.1093/brain/114.5.2283>
- Filippi, M., Basaia, S., Sarasso, E., Stojkovic, T., Stankovic, I., Fontana, A., Tomic, A., Piramide, N., Stefanova, E., Markovic, V., Kostic, V. S., & Agosta, F. (2020). Longitudinal brain connectivity changes and clinical evolution in Parkinson's disease. *Molecular Psychiatry*, 26, 5429–5440. <https://doi.org/10.1038/s41380-020-0770-0>
- Gabrieli, J. D., Poldrack, R. A., & Desmond, J. E. (1998). The role of left prefrontal cortex in language and memory. *Proceedings of the National Academy of Sciences of the United States of America*, 95(3), 906–913. <https://doi.org/10.1073/pnas.95.3.906>
- Galvan, A., & Wichmann, T. (2008). Pathophysiology of parkinsonism. *Clinical Neurophysiology*, 119(7), 1459–1474. <https://doi.org/10.1016/j.clinph.2008.03.017>
- Goedert, M., Masuda-Suzukake, M., & Falcon, B. (2017). Like prions: The propagation of aggregated tau and alpha-synuclein in neurodegeneration. *Brain*, 140(2), 266–278. <https://doi.org/10.1093/brain/aww230>
- Hamilton, M. (1959). The assessment of anxiety states by rating. *The British Journal of Medical Psychology*, 32(1), 50–55. <https://doi.org/10.1111/j.2044-8341.1959.tb00467.x>
- Hoehn, M. M., & Yahr, M. D. (1967). Parkinsonism: Onset, progression and mortality. *Neurology*, 17(5), 427–442. <https://doi.org/10.1212/wnl.17.5.427>
- Hou, Y., Luo, C., Yang, J., Ou, R., Song, W., Wei, Q., Cao, B., Zhao, B., Wu, Y., Shang, H. F., & Gong, Q. (2016). Prediction of individual clinical scores in patients with Parkinson's disease using resting-state functional magnetic resonance imaging. *Journal of the Neurological Sciences*, 366, 27–32. <https://doi.org/10.1016/j.jns.2016.04.030>
- Hu, X. F., Zhang, J. Q., Jiang, X. M., Zhou, C. Y., Wei, L. Q., Yin, X. T., Li, J., Zhang, Y. L., & Wang, J. (2015). Amplitude of low-frequency oscillations in Parkinson's disease: A 2-year longitudinal resting-state functional magnetic resonance imaging study. *Chinese Medical Journal*, 128(5), 593–601. <https://doi.org/10.4103/0366-6999.151652>
- Hughes, A. J., Daniel, S. E., Kilford, L., & Lees, A. J. (1992). Accuracy of clinical diagnosis of idiopathic Parkinson's disease: A clinico-pathological study of 100 cases. *Journal of Neurology, Neurosurgery, and Psychiatry*, 55(3), 181–184. <http://www.ncbi.nlm.nih.gov/pubmed/1564476>
- Iwaki, H., Blauwendraat, C., Leonard, H. L., Makarios, M. B., Kim, J. J., Liu, G., Maple-Groden, J., Corvol, J. C., Pihlstrom, L., van Nimwegen, M., Smolensky, L., Amondikar, N., Hutten, S. J., Frasier, M., Nguyen, K. H., Rick, J., Eberly, S., Faghri, F., Auinger, P., ... Nalls, M. A. (2021). Differences in the presentation and progression of Parkinson's disease by sex. *Movement Disorders*, 36(1), 106–117. <https://doi.org/10.1002/mds.28312>
- Jenkinson, C., Peto, V., Fitzpatrick, R., Greenhall, R., & Hyman, N. (1995). Self-reported functioning and well-being in patients with Parkinson's disease: Comparison of the short-form health survey (SF-36) and the Parkinson's disease questionnaire (PDQ-39). *Age and Ageing*, 24(6), 505–509. <https://doi.org/10.1093/ageing/24.6.505>
- Jia, X.-Z., Zhao, N., Dong, H.-M., Sun, J.-W., Barton, M., Burciu, R., Carrière, N., Cerasa, A., Chen, B.-Y., Chen, J., Coombes, S., Defebvre, L., Delmaire, C., Dujardin, K., Esposito, F., Fan, G.-G., Di Nardo, F., Feng, Y.-X., Fling, B. W., ... Zang, Y.-F. (2021). Small P values may not yield robust findings: An example using REST-meta-PD. *Science Bulletin*, 66(21), 2148–2152. <https://doi.org/10.1016/j.scib.2021.06.007>
- Li, K., Su, W., Chen, M., Li, C. M., Ma, X. X., Wang, R., Lou, B. H., Zhao, H., Chen, H. B., & Yan, C. Z. (2020). Abnormal spontaneous brain activity in left-onset Parkinson disease: A resting-state functional MRI study. *Frontiers in Neurology*, 11, 727. <https://doi.org/10.3389/fneur.2020.00727>
- Luo, C., Guo, X., Song, W., Chen, Q., Yang, J., Gong, Q., & Shang, H. F. (2015). The trajectory of disturbed resting-state cerebral function in Parkinson's disease at different Hoehn and Yahr stages. *Human Brain Mapping*, 36(8), 3104–3116. <https://doi.org/10.1002/hbm.22831>
- Luo, C., Song, W., Chen, Q., Zheng, Z., Chen, K., Cao, B., Yang, J., Li, J., Huang, X., Gong, Q., & Shang, H. F. (2014). Reduced functional connectivity in early-stage drug-naive Parkinson's disease: A resting-state fMRI study. *Neurobiology of Aging*, 35(2), 431–441. <https://doi.org/10.1016/j.neurobiolaging.2013.08.018>
- Marras, C., & Lang, A. (2013). Parkinson's disease subtypes: Lost in translation? *Journal of Neurology, Neurosurgery, and Psychiatry*, 84(4), 409–415. <https://doi.org/10.1136/jnnp-2012-303455>
- Meppelink, A. M., de Jong, B. M., Renken, R., Leenders, K. L., Cornelissen, F. W., & van Laar, T. (2009). Impaired visual processing preceding image recognition in Parkinson's disease patients with visual hallucinations. *Brain*, 132(Pt 11), 2980–2993. <https://doi.org/10.1093/brain/awp223>
- Miller, E. K., & Cohen, J. D. (2001). An integrative theory of prefrontal cortex function. *Annual Review of Neuroscience*, 24, 167–202. <https://doi.org/10.1146/annurev.neuro.24.1.167>
- Moberg, P. J., Lazarus, L. W., Meshulam, R. I., Bilker, W., Chuy, I. L., Neyman, I., & Markvart, V. (2001). Comparison of the standard and structured interview guide for the Hamilton depression rating scale in depressed geriatric inpatients. *The American Journal of Geriatric Psychiatry*, 9(1), 35–40. <https://www.ncbi.nlm.nih.gov/pubmed/11156750>
- Movement Disorder Society Task Force on Rating Scales for Parkinson's D. (2003). The unified Parkinson's disease rating scale (UPDRS): Status and recommendations. *Movement Disorders*, 18(7), 738–750. <https://doi.org/10.1002/mds.10473>
- Nagano-Saito, A., Al-Azzawi, M. S., Hanganu, A., Degroot, C., Mejia-Constain, B., Bedetti, C., Lafontaine, A. L., Soland, V., Chouinard, S., & Monchi, O. (2016). Patterns of longitudinal neural activity linked to different cognitive profiles in Parkinson's disease. *Frontiers in Aging Neuroscience*, 8, 275. <https://doi.org/10.3389/fnagi.2016.00275>
- Nasreddine, Z. S., Phillips, N. A., Bedirian, V., Charbonneau, S., Whitehead, V., Collin, I., Cummings, J. L., & Chertkow, H. (2005). The Montreal cognitive assessment, MoCA: A brief screening tool for mild cognitive impairment. *Journal of the American Geriatrics Society*, 53(4), 695–699. <https://doi.org/10.1111/j.1532-5415.2005.53221.x>
- Nguyen, K. P., Raval, V., Treacher, A., Mellema, C., Yu, F. F., Pinho, M. C., Subramaniam, R. M., Dewey, R. B., Jr., & Montillo, A. A. (2021). Predicting Parkinson's disease trajectory using clinical and neuroimaging baseline measures. *Parkinsonism & Related Disorders*, 85, 44–51. <https://doi.org/10.1016/j.parkreldis.2021.02.026>
- Ou, R., Wei, Q., Hou, Y., Zhang, L., Liu, K., Lin, J., Jiang, Z., Song, W., Cao, B., & Shang, H. (2021a). Effect of diabetes control status on the progression of Parkinson's disease: A prospective study. *Annals of*

- Clinical Translational Neurology*, 8(4), 887–897. <https://doi.org/10.1002/acn3.51343>
- Ou, R., Wei, Q., Hou, Y., Zhang, L., Liu, K., Lin, J., Jiang, Z., Zhao, B., Cao, B., & Shang, H. (2021b). Facial tremor in patients with Parkinson's disease: Prevalence, determinants and impacts on disease progression. *BMC Neurology*, 21(1), 86. <https://doi.org/10.1186/s12883-021-02105-y>
- Pan, P., Zhang, Y., Liu, Y., Zhang, H., Guan, D., & Xu, Y. (2017). Abnormalities of regional brain function in Parkinson's disease: A meta-analysis of resting state functional magnetic resonance imaging studies. *Scientific Reports*, 7, 40469. <https://doi.org/10.1038/srep40469>
- Picillo, M., Nicoletti, A., Fetoni, V., Garavaglia, B., Barone, P., & Pellicchia, M. T. (2017). The relevance of gender in Parkinson's disease: A review. *Journal of Neurology*, 264(8), 1583–1607. <https://doi.org/10.1007/s00415-016-8384-9>
- Possin, K. L., Kang, G. A., Guo, C., Fine, E. M., Trujillo, A. J., Racine, C. A., Wilhelm, R., Johnson, E. T., Witt, J. L., Seeley, W. W., Miller, B. L., & Kramer, J. H. (2013). Rivastigmine is associated with restoration of left frontal brain activity in Parkinson's disease. *Movement Disorders*, 28(10), 1384–1390. <https://doi.org/10.1002/mds.25575>
- Postuma, R. B., Berg, D., Stern, M., Poewe, W., Olanow, C. W., Oertel, W., Obeso, J., Marek, K., Litvan, I., Lang, A. E., Halliday, G., Goetz, C. G., Gasser, T., Dubois, B., Chan, P., Bloem, B. R., Adler, C. H., & Deuschl, G. (2015). MDS clinical diagnostic criteria for Parkinson's disease. *Movement Disorders*, 30(12), 1591–1601. <https://doi.org/10.1002/mds.26424>
- Ranstam, J., & Cook, J. A. (2018). LASSO regression. *British Journal of Surgery*, 105(10), 1348. <https://doi.org/10.1002/bjs.10895>
- Shulman, L. M., Gruber-Baldini, A. L., Anderson, K. E., Fishman, P. S., Reich, S. G., & Weiner, W. J. (2010). The clinically important difference on the unified Parkinson's disease rating scale. *Archives of Neurology*, 67(1), 64–70. <https://doi.org/10.1001/archneurol.2009.295>
- Tomlinson, C. L., Stowe, R., Patel, S., Rick, C., Gray, R., & Clarke, C. E. (2010). Systematic review of levodopa dose equivalency reporting in Parkinson's disease. *Movement Disorders*, 25(15), 2649–2653. <https://doi.org/10.1002/mds.23429>
- Tzourio-Mazoyer, N., Landeau, B., Papathanassiou, D., Crivello, F., Etard, O., Delcroix, N., Mazoyer, B., & Joliot, M. (2002). Automated anatomical labeling of activations in SPM using a macroscopic anatomical parcellation of the MNI MRI single-subject brain. *NeuroImage*, 15(1), 273–289. <https://doi.org/10.1006/nimg.2001.0978>
- Wang, G., Hong, Z., Cheng, Q., Xiao, Q., Wang, Y., Zhang, J., Ma, J. F., Wang, X. J., Zhou, H. Y., & Chen, S. D. (2009). Validation of the Chinese non-motor symptoms scale for Parkinson's disease: Results from a Chinese pilot study. *Clinical Neurology and Neurosurgery*, 111(6), 523–526. <https://doi.org/10.1016/j.clineuro.2009.02.005>
- Wang, J., Zhang, J. R., Zang, Y. F., & Wu, T. (2018). Consistent decreased activity in the putamen in Parkinson's disease: A meta-analysis and an independent validation of resting-state fMRI. *Gigascience*, 7(6), giy071. <https://doi.org/10.1093/gigascience/giy071>
- Wang, Z., Jia, X., Chen, H., Feng, T., & Wang, H. (2018). Abnormal spontaneous brain activity in early Parkinson's disease with mild cognitive impairment: A resting-state fMRI study. *Frontiers in Physiology*, 9, 1093. <https://doi.org/10.3389/fphys.2018.01093>
- Yuan, P., & Raz, N. (2014). Prefrontal cortex and executive functions in healthy adults: A meta-analysis of structural neuroimaging studies. *Neuroscience and Biobehavioral Reviews*, 42, 180–192. <https://doi.org/10.1016/j.neubiorev.2014.02.005>
- Zeighami, Y., Fereshtehnejad, S. M., Dadar, M., Collins, D. L., Postuma, R. B., & Dagher, A. (2019). Assessment of a prognostic MRI biomarker in early de novo Parkinson's disease. *NeuroImage Clin*, 24, 101986. <https://doi.org/10.1016/j.nicl.2019.101986>
- Zhang, J., Wei, L., Hu, X., Zhang, Y., Zhou, D., Li, C., Wang, X., Feng, H., Yin, X., Xie, B., & Wang, J. (2013). Specific frequency band of amplitude low-frequency fluctuation predicts Parkinson's disease. *Behavioural Brain Research*, 252, 18–23. <https://doi.org/10.1016/j.bbr.2013.05.039>
- Zou, Q. H., Zhu, C. Z., Yang, Y., Zuo, X. N., Long, X. Y., Cao, Q. J., Wang, Y. F., & Zang, Y. F. (2008). An improved approach to detection of amplitude of low-frequency fluctuation (ALFF) for resting-state fMRI: Fractional ALFF. *Journal of Neuroscience Methods*, 172(1), 137–141. <https://doi.org/10.1016/j.jneumeth.2008.04.012>

SUPPORTING INFORMATION

Additional supporting information can be found online in the Supporting Information section at the end of this article.

How to cite this article: Hou, Y., Zhang, L., Ou, R., Wei, Q., Gu, X., Liu, K., Lin, J., Yang, T., Xiao, Y., Gong, Q., & Shang, H. (2023). Motor progression marker for newly diagnosed drug-naïve patients with Parkinson's disease: A resting-state functional MRI study. *Human Brain Mapping*, 44(3), 901–913. <https://doi.org/10.1002/hbm.26110>